Investigating the path of light in a medium with continuously changing refractive index.

Samuel Josephs
L2 Lab Skills and Electronics, Lab Group 3, Thursday
Submitted: March 25, 2022, Date of Experiment: 10/01/2022 - 25/03/2022

In this experiment the curved path a beam of light takes in a medium with continuously changing refractive index is explained from first principles using Maxwell's equations. Using data of the path obtained programmatically the distribution of refractive index as a function of height is obtained.

I. INTRODUCTION

FIG. 1: Image of laser entering at $\pi/2$ radians to the vertical axis from the left.

When light propagates through a medium with constantly changing refractive index a curved path is traversed as observed in **FIG.1**. In this experiment a concentration gradient of sugar induces the change in refractive index (n), sugar has a high relative permittivity [3] (ϵ_r). As $n = \sqrt{\epsilon_r}$ for constant relative permeability the sugar contributes to the refractive index in the water. There are two explanations for this phenomena, the first being derived from Maxwell's equations and the second being derived from Fermat's principle which states that "light travels between two points along the path that extremises time, as compared to other nearby paths.".

This effect is observed in the atmosphere as the refractive index of air is a function of density which decreases with altitude. However this effect is drowned out by interaction with the ionosphere at high altitudes. This effect results in an increased range of radio communications extending the effective radius of the earth to about[1] $\frac{4}{3}$ what it would be without this effect. As such satellites must take this effect into account when sending data to the surface of the earth. Planes must also factor this in when communicating with air traffic control.

A. Maxwell's Equations

Maxwell's equations are a complete description of electromagnetic phenomena such as light. They can be written as follows:

$$\nabla \cdot \vec{E} = \frac{\rho}{\epsilon_0} \tag{1}$$

$$\nabla \cdot \vec{B} = 0 \tag{2}$$

$$\nabla \times \vec{E} = -\frac{\partial \vec{B}}{\partial t} \tag{3}$$

$$\nabla \times \vec{B} = \mu_0 \vec{J} + \mu_0 \epsilon_0 \frac{\partial \vec{E}}{\partial t} \tag{4}$$

Taking the curl of Maxwell's third equation, substituting in Maxwell's fourth equation and setting $J = \frac{\partial \vec{P}}{\partial t}$ where $\vec{P} = \epsilon_0(\epsilon_r - 1)\vec{E}$ (Which is the case for a dielectric medium) yields

$$\nabla^2 \vec{E} = \mu_0 \epsilon_0 \epsilon_r \frac{\partial^2 \vec{E}}{\partial t^2} = \frac{n^2}{c^2} \frac{\partial^2 \vec{E}}{\partial t^2} \tag{5}$$

This is a wave equation that in theory completely describes the propagation of light through a dielectric medium. However an analytic solution for the path cannot be directly obtained.
First as the path is time invariant the time and spatial components shall be separated out such that $E(x, y, t) = F(x, y)T(t)$

$$\frac{1}{n^2 F}\nabla^2 F = \frac{\partial^2 T}{\partial t^2}\frac{1}{c^2 T} = -k^2 \tag{6}$$

$$\nabla^2 F + k^2 n^2 F = 0 \tag{7}$$

Equation 7 is known as the Helmholtz equation. Next solutions of the form

$$E = E_0 e^{-ikS(r)} \tag{8}$$

shall be assumed. Here a scalar approximation has been made and the function $S(r)$ describes the phase at a given coordinate r. As such it is worth noting that

$$\nabla S(r) \propto \frac{d\vec{r}}{ds}$$

where $ds^2 = dx^2 + dy^2$ and the right hand side is the tangent to the path.
Substituting into equation 8 the following is obtained

$$\nabla^2 E_0 - k^2 |\nabla S|^2 E_0 + k^2 n^2 E_0 - ik\nabla^2 S = 0 \tag{9}$$

Setting the real components to zero

$$|\nabla S|^2 = n^2 + \frac{\nabla^2 E_0}{k^2 E_0} \tag{10}$$

making the approximation that $n^2 >> \frac{\nabla^2 E_0}{k^2 E_0}$ (which is valid for rays) gives us the Eikonal equation

$$|\nabla S| = n \tag{11}$$

The Eikonal equation describes how a ray propagates. taking the gradient of both sides

$$\nabla |\nabla S| = \nabla n \tag{12}$$

$$\nabla \left| \begin{pmatrix} \frac{dS}{dx} \\ \frac{dS}{dy} \end{pmatrix} \right| = \nabla n \tag{13}$$

$$\nabla \sqrt{\left(\frac{dS}{dx}\right)^2 + \left(\frac{dS}{dy}\right)^2} = \nabla n \tag{14}$$

$$\frac{d}{ds}\nabla S = \frac{d}{ds}\lambda \frac{d\vec{r}}{ds} = \nabla n \tag{15}$$

Where A is a constant. Solving equation 15 will give the path of the ray. Assuming $n(y) = my + c$ equation 15 becomes

$$\frac{d}{ds}\lambda\frac{dx}{ds} = 0 \rightarrow \lambda\frac{dx}{ds} = A \tag{16}$$

$$\frac{d}{ds}\lambda\frac{dy}{dx}\frac{dx}{ds} = m \rightarrow A\frac{d^2y}{dx^2} = m\sqrt{1+y'^2}dx \tag{17}$$

Integrating both sides of equation 17 twice noting that $cosh^2 = 1 + sinh^2$ gives a formula for the path

$$y = \frac{A}{m}cosh\left(\frac{m(x-x_0)}{A}\right) + y_0 \tag{18}$$

B. Fermat's principle

To describe the path using Fermat's principle first an expression for the time must be constructed

$$dT = \frac{\text{distance}}{\text{velocity}} = \frac{\sqrt{dx^2+dy^2}}{V(y)} = \frac{n(y)\sqrt{1+y'^2}}{c}dx \tag{19}$$

From this the total time $T(y)$ can be expressed as

$$T(y) = \frac{1}{c}\int_{x_1}^{x_2} n(y)\sqrt{1+y'^2}dx \tag{20}$$

Equation 20 is a convex function as time can only increase, therefore we can use the Legendre transform such that

$$n(y)\sqrt{1+y'^2} + H = y'\frac{d}{dy}n(y)\sqrt{1+y'^2} \tag{21}$$

$$H = y'\frac{d}{dy'}n(y)\sqrt{1+y'^2} + n(y)\sqrt{1+y'^2} \tag{22}$$

$$\frac{dy}{dx} = \sqrt{\frac{n(y)^2}{H^2} - 1} = \frac{1}{H}\sqrt{n(y)^2 - H^2} \tag{23}$$

As H is only a function of y and y' $\frac{dH}{dx} = 0$ thus H is constant. From a geometric argument the derivative is equal to $cot(\theta)$ where θ is the angle between the horizontal axis and the tangent to the path. Thus H must be a constant not dependant on y. Rearranging equation 23

$$\frac{n}{H} = \sqrt{\left(\frac{dy}{dx}\right)^2 + 1} \tag{24}$$

this will allow the calculation of a constant multiplied by n from data as shown in **FIG.4**.

II. METHODS

A fish tank was filled with warm tap water and green food dye was poured in. the food dye scatters the laser making it's path visible. The water was then stirred to dissolve the food dye uniformly through the water then the water was allowed to come to rest over the course of 15 minutes. Granulated sugar was then poured in very quickly such that it formed a thin layer on the bottom of the tank. The heater was turned on next to the tank and the setup was left over night. After twenty four hours have passed the layer of sugar on the bottom of the tank will have dissolved and the laser will be able to reflect off of the bottom. We used a sub $1mW$ laser to avoid any danger of eye damage.

A program [2] was used to extract the path of the laser from an image of the experiment such as that shown in **FIG.1**. This program gives around 2000 data points, from these data points the mean of every four was taken to reduce noise which allows the numerical derivative to be calculated for the middle bounce as shown in **FIG.2**. The middle bounce was chosen as it is the largest portion of the data and the models do not account for reflection off of the bottom of the tank. Equation 24 was then used used to compute $\frac{n(y)}{H}$ from this data, this is shown in **FIG.4**

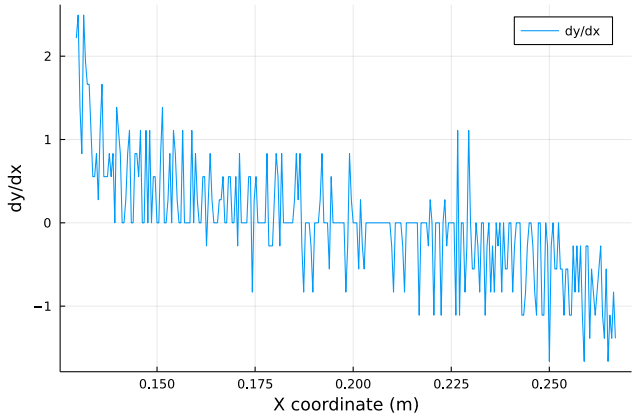

FIG. 2: Gradient of middle bounce. The x axis is the horizontal coordinate and the y axis is the numerically calculated derivative.

III. RESULTS

Model	Minimised Chi Squared	A	m
$\frac{n}{H} = my + c$	1.29	N/A	-4.57×10^{-7}
$\frac{n}{H} = Ae^{-my} + c$	1.06	3.69×10^{-8}	300

The above table shows the minimised chi squared of various test functions shown in **FIG.4**. The optimal values of the parameters in equation 18 were found and are displayed in the following table.

Graph	A	m	$x_0(m)$	$y_0(m)$
FIG.3a	0.0292	$-0.268 \pm 5 \times 10^{-4}$	$0.197 \pm 5 \times 10^{-4}$	0.136
FIG.3b	0.0292	$-0.267 \pm 5 \times 10^{-4}$	$0.197 \pm 5 \times 10^{-4}$	0.136

The uncertainties are ± 0.00005 for A and $\pm 0.0005m$ y_0.

IV. DISCUSSION

A. Evaluating Model Accuracy

As seen in **FIG.4** a linear distribution is a reasonable estimation with a chi squared of 1.38, this is especially true for values not near the bottom. As such it would be expected that equation 18 would fit well for values not near the bottom (At the centre of the bounce), but terribly for values near the bottom (At either edge of the bounce) where the distribution becomes very exponential or reciprocal as seen in **FIG.4**. This is confirmed by **FIG.3a** which fits poorly with a reduced chi squared of 19.5, and **FIG.3b** which is a good fit with a reduced chi squared of 1.34. Thus

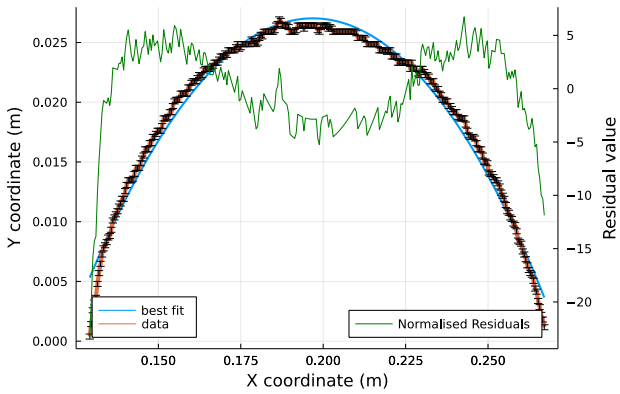

(a) Graph of data from entire middle bounce, the reduced chi squared is 17.1 and the Durbin-Watson statistic is 0.067. The residuals have a mean of 2.12×10^{-6} and a standard deviation of 4.11

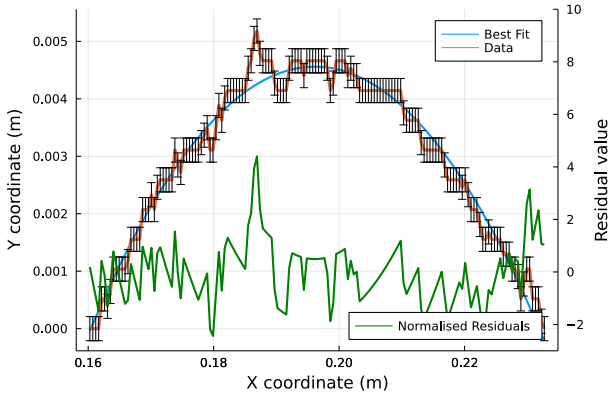

(b) Graph of fitted data from the centre of the bounce. The reduced chi squared is 1.27 and the Durbin-Watson statistic is 0.58. The residuals have a mean of -2.32×10^{-6} and a standard deviation of 1.11

FIG. 3: Graphs of the data from experiments obtained from images such as **FIG.1**

using an image analysis program[2]. The line of best fit is a fitted version of equation 18 and is plotted alongside the normalised residuals.

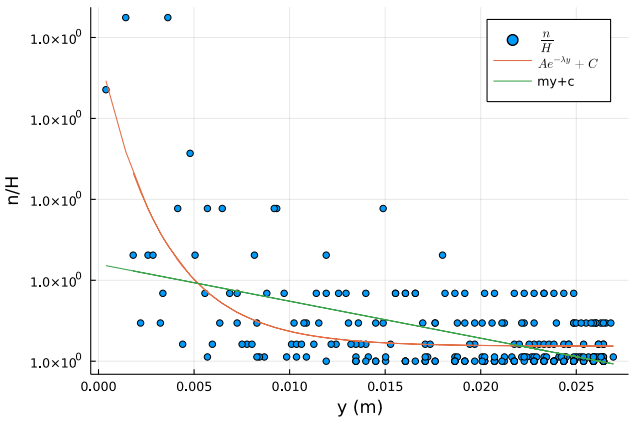

FIG. 4: The distribution of n plotted against the vertical pixel position scaled to cm using the measured height of water in the tank (10.05 ± 0.005cm) using equation 24

.

equation 18 is a suitable approximation for parts of the curve not near the bottom and equation 15 is an accurate description for the entire curve.

Sugar is a very strong dielectric[3], as such it should be possible to relate the distribution of the relative permittivity to the refractive index.

$$n = \frac{c}{v} = \frac{\sqrt{\mu_0 \epsilon_0 \epsilon_r}}{\sqrt{\mu_0 \epsilon_0}} = \sqrt{\epsilon_r} \rightarrow \epsilon_r = n^2 \tag{25}$$

Assuming no relative magnetic permeability μ_r.

By substituting in $n = my + c$ such that equation 18 is expected as shown in **FIG.3b**

$$\epsilon_r = (my + c)^2 = m^2 y^2 + 2mcy + c^2 \tag{26}$$

This is a decent approximation but predicts that the relative permittivity will initially decrease, reach zero, then increase again. This cannot be true as it would predict the concentration of sugar would decrease then increase as y increases which is not what is observed. As such it would be worthwhile to try other models on **FIG.4**.

The first issue encountered is that whilst the parameters on the right hand side of the models in **FIG.4** can be calculated the value of H is unknown. to calculate an approximate value of H equate the equations

$$m_1 y + c_1 = H(m_2 y + c_2) \tag{27}$$

$$H = \frac{m_1 y + c_1}{m_2 y + c_2} \tag{28}$$

now the issue is that c_1 is unknown. As equation 15 shows that c_1 and c_2 should have no effect on the path taken, they can both be set to zero.

$$H \approx \frac{m_1}{m_2} = \frac{-4.57 \times 10^{-7}}{-2.68 \times 10^{-4}} = \frac{457}{268000} \tag{29}$$

From this an approximate forms for the refractive index could be the following exponential form

$$n = H\left(3.89 \times 10^{-8} e^{-300y} + 1\right) \tag{30}$$

Putting these into equation 25

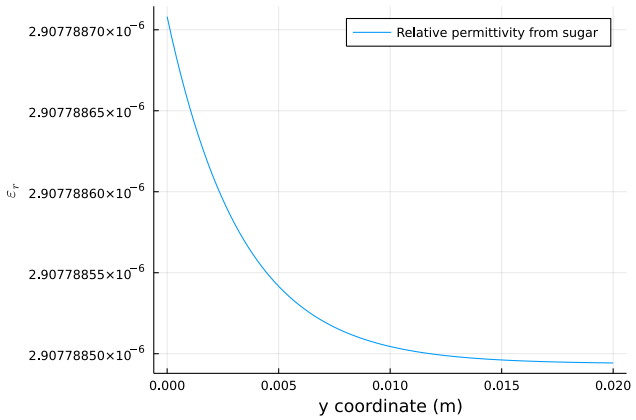

FIG. 5: Graph of relative permittivity predicted by equation 30.

The issue with **FIG.5** is that it does not take into account the dielectric properties of the water it is dissolved in and

as water's relative permittivity is similar to that of sugar will be inaccurate but it is likely to give the correct shape of the distribution.

The Durbin-Watson statistic of **FIG.3a** and **FIG.3b** are both much less than 2. Between 1.5-2.5 is considered normal but as they are both much less than one this shows a high degree of positive autocorrelation, meaning that each previous residual point can predict the next. In the case of **FIG.3a** this can be explained by the the theory as the assumption of linear n is shown in **FIG.4** to be false. As the model does not fit in a symmetrical manner it makes sense that there is high autocorrelation.
This is more puzzling for **FIG.3b** as the residuals seem on first look to be randomly distributed with a single large spike in the centre. One possibility is that due to the data being collected from an image means that it is discretely, and so predictably distributed. Though when looking at the normalised residuals they are approximately normally distributed with a mean of 0 and standard deviation of 1 which is what would be expected for a model that fitted the data well.

B. Improvements

There are various sources of uncertainty and noise in the experimental setup that can be reduced. The main source of uncertainty is the quality of camera used to take a picture of the experiment. We used a standard phone camera of a Motorola E series Samsung A21s. Due to how the program[2] that processes the image works a high contrast between the scattered laser light and background is desired. To achieve this photos were taken at night with all lights off, the phone camera struggled in these environments resulting in many blurred images increasing the uncertainty in the position of the beam. A better quality night vision camera would be very beneficial in reducing uncertainty.

Other measurements that could be taken is the dependence of frequency on the path taken by the laser. Due to the nature of how lasers generate light this would require a variety of lasers generating different frequencies of light. As the relative permittivity ϵ_r is a function of angular frequency

$$\epsilon_{r,\text{Real}} = 1 + \frac{Nq^2}{m\epsilon_0} \frac{w_0^2 - w^2}{(w_0^2 - w^2)^2 + \left(\frac{w}{\tau}\right)^2} \tag{31}$$

$$\epsilon_{r,\text{Imaginary}} = \frac{Nq^2}{m\epsilon_0 \tau} \frac{w}{(w_0^2 - w^2)^2 + \left(\frac{w}{\tau}\right)^2} \tag{32}$$

and since $n = \sqrt{\epsilon_r}$ it is clear that a change in frequency should change the refractive index and so the path taken by the laser.
Equations 31 and 32 are obtained from the Drude model of matter. τ is the average time between electron-ion collisions, N is the dipole number density, q is the dipole charge, m is the mass of each molecule that forms each end of the dipole, and $w = 2\pi f$.

FIG.4 and **FIG.5** could be validated by use of a refractometer. This device would allow samples to be taken from various heights in the tank and the refractive index measured. However a method would have to be created to obtain these samples with minimal disturbance to the medium in the tank, as any disturbance will mix the sugar into the water destroying the concentration gradient locally, which would quickly cause diffusion to disturb the concentration gradient in the entire tank.

It would be worthwhile to measure the polarization at the entry and exit points of the tank to see how propagating through the tank changes the polarization of the light. As sugar is a chiral molecule it would be expected to have some effect.

V. CONCLUSIONS

For a concentration gradient of sugar in water the path a light beam will take is given by equation 18 and resembles a catenary curve at the top of the bounce as shown in **FIG.3b**. The path can also be fully described by differential equations 15 and 23. The distribution of refractive index as a function of height can be modelled by a function of exponential decay as shown in **FIG.4**.

Acknowledgments

I would like to thank Professor Damian Hampshire for prompting me towards an analytic solution for the path of the laser from Maxwell's equations.

References

[1] Christopher Haslett. Essentials of radio wave propagation, pp 119–120. Cambridge University, 2008.
[2] Samuel Josephs. Laser image processor. https://github.com/SamuelJosephs/Laser_image_processor, February 2022.
[3] T.N. Tulasidas, Vijaya Raghavan, F.van Voort, and Réjean Girard. Dielectric properties of grapes and sugar solutions at 2.45 ghz. The Journal of microwave power and electromagnetic energy : a publication of the International Microwave Power Institute, 30:117–23, 02 1995.

Error Appendix

Errors were calculated to be half the vertical height of the beam in pixels, then scaled using the height of the picture to convert into meters. Parallax will make a significant contribution to errors especially in the horizontal axis. In order to minimise this pictures were taken from the centre of the tank. Due to the nature of data being gathered from a single image there are very few sources of errors, other than parallax the only other sources of error are the entry height of the laser into the tank (which was measured with a ruler but never used), the height of the water in the tank and how level the tank is. A key assumption in our modeling is that the normal to the floor of the tank is parallel to the gravitational field lines. The only available table that was used for this experiment is far from guaranteed to be flat, if this experiment was repeated a spirit level should be used to quantify an error associated with the flatness of the surface.

The height of water in the tank is important as to eliminate background noise from reflections and scale the pixel data into physical dimensions. The image was cropped such that only the entire length of the tank and height of the water was processed. the pixel data was then scaled using this width and height. The width was taken from the manufacturers specifications and the height of the water was measured with a ruler.

Another source of error is the pitch, yaw, and roll of the camera at the moment the picture is taken. The roll was minimised by placing the camera on a laboratory scissor jack. This allowed for increased repeatability between pictures as all pictures would be taken from the same position and same roll angle.

All errors were propagated in line with Measurements and their Uncertainties by Hughes and Hayes.

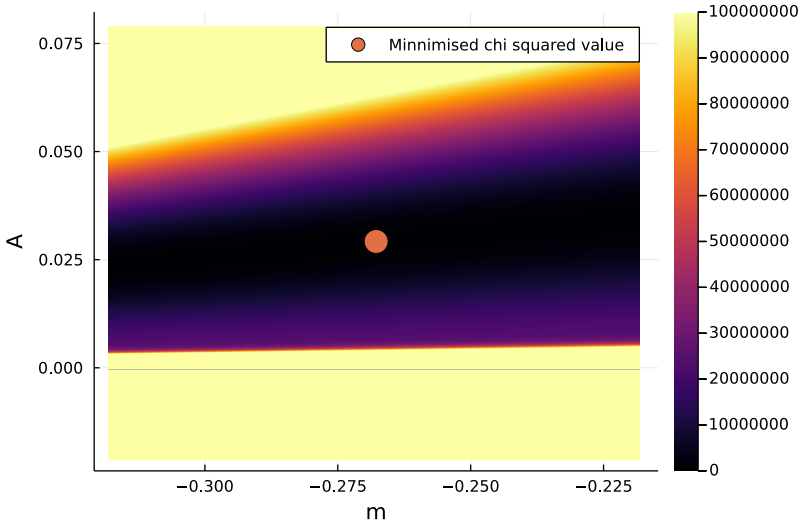

FIG. 6: Heatmap of chi squared values for equation 18

In the above heatmap it can be seen that there is a valley of chi squared values with the minnimised value at one point in this valley. Looking at equation 18 it can be seen that it is only the ratio $\frac{A}{m}$ that contributes to the chi squared value.

Equation 18 can be rewritten as

$$y = Kcosh\left(\frac{(x - x_0)}{K}\right) + y_0 \tag{33}$$

Where $K = \frac{A}{m}$. This explains the valley in the heat map. x_0 is the horizontal coordinate of the maximum or minimum of the path and as such can be experimentally determined as well as computed by using gradient descent on the model's chi squared. y_0 is a constant of integration and so is dependant on our choice of coordinates and is determined by initial conditions before the first bounce and after the second bounce. In the middle bounce it can be determined by the maxima or minima vertical coordinate or like x_0 by gradient descent. In this experiment gradient descent was used as initial conditions are not of interest, rather we only wanted to test if various models could predict the path and measuring initial conditions would have very large uncertainties for the middle bounce (where the vast majority of the data is) as we would have to measure the initial gradient at the reflection point, the horizontal distance of the first and second reflection points and the vertical distance of the entry and exit points. Then propagate these errors when computing the values of x_0 and y_0.

Scientific Summary for a General Audience

When light enters a different medium it can change direction, this effect is observable in many places such as swimming pools. But why does this happen? The explanation many will have come across before is that there is a change in refractive

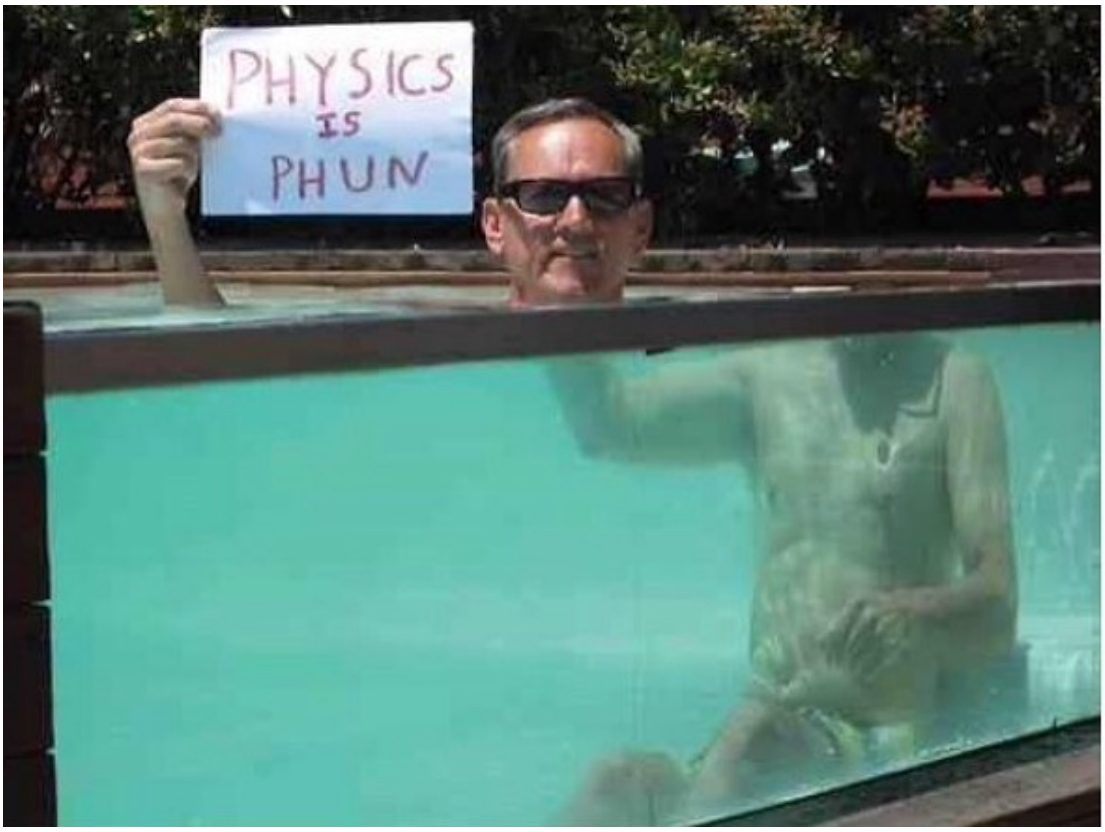

FIG. 7: Demonstration of refraction in a swimming pool, the man hasn't actually lost his literal mind!

index between the air and water. Whilst this is true it doesn't give much intuition as to what is going on, so what exactly is refractive index?

$$n = \frac{c}{v_{\text{Group}}} \tag{34}$$

The equation above is the definition of refractive index, it states that refractive index (n) is the speed of light in a vacuum (c) (e.g. space) divided by the speed of light in the material we are interested. This means that light slows down* when it enters a medium with a higher refractive index! This is what causes the change in direction.

In our experiment the refractive index is constantly changing thus the light is constantly changing direction forming a curve.

*: Those who are familiar with the premise of special relativity may find this statement confusing, as surely the speed of light is the same everywhere? What goes on is that light's oscillating electric field causes electrons in the material to accelerate. These electrons create their own wave whose effects when added on to the original light wave create a new wave that appears to travel with a lower velocity. The velocity of this group of waves is called the group velocity! This is seen in equation 34.